ResearchGate

See discussions, stats, and author profiles for this publication at: https://www.researchgate.net/publication/49761331

Single molecules reveal the dynamics of heterogeneities in a polymer at the glass transition

ARTICLE *in* THE JOURNAL OF CHEMICAL PHYSICS · JANUARY 2011

Impact Factor: 2.95 · DOI: 10.1063/1.3516516 · Source: PubMed

CITATIONS
16

READS
20

3 AUTHORS, INCLUDING:

Dieter Bingemann
Williams College
14 PUBLICATIONS **297** CITATIONS
SEE PROFILE

Scott Olesen
Massachusetts Institute of Technology
2 PUBLICATIONS **21** CITATIONS
SEE PROFILE

Available from: Dieter Bingemann
Retrieved on: 24 January 2016

Single molecules reveal the dynamics of heterogeneities in a polymer at the glass transition

Dieter Bingemann,[a] Rachel M. Allen,[b] and Scott W. Olesen
Department of Chemistry, Williams College, 47 Lab Campus Drive, Williamstown, Massachusetts 01267, USA

(Received 24 February 2010; accepted 26 October 2010; published online 11 January 2011)

The notion of heterogeneous dynamics in glasses, that is, the spatial and temporal variations of structural relaxation rates, explains many of the puzzling features of glass dynamics. The nature and the dynamics of these heterogeneities, however, have been very controversial. Single rhodamine B molecules in poly(vinyl acetate) at the glass transition reorient through sudden jumps. With a statistical search for the most likely break points in the logarithm of the ratio of the two perpendicular fluorescence polarizations, we determine the times of these angular jumps. We interpret these jumps as an indication for individual glass rearrangements in the vicinity of the probe molecule. Time-series analysis of the resulting sequence of waiting times between jumps shows that dynamic heterogeneities in the matrix exist, but are short lived. From the correlation of the logarithm of the waiting time between subsequent jumps, we determine an upper limit for the lifetime of heterogeneities in the sample. The correlation time of $\tau_{\text{het}} = 32$ s is three times shorter than the orientational correlation time of the probe molecule, $\tau_{\text{orient}} = 90$ s, in the sample at this temperature, but 13 times longer than the structural relaxation time, $\tau_\alpha = 2.5$ s, estimated for this sample from dielectric experiments. We present a model for glass dynamics in which each rearrangement in one region causes a random change in the barrier height for subsequent rearrangements in a neighboring region. This model, which equates the dynamics of the heterogeneities with the dynamics of the glass itself and thus implies a factor of one between heterogeneity lifetime and structural relaxation time, successfully reproduces the statistics of the experimentally observed waiting time sequences. © *2011 American Institute of Physics*. [doi:10.1063/1.3516516]

I. INTRODUCTION

Most liquids, when cooled well below their freezing point without crystallization, rapidly become very viscous until, at the glass transition temperature, they behave like a solid.[1,2] Surprisingly, no structural change has been identified in the material during this transition from supercooled liquid to glass.[3] Despite the widespread use of glasses and supercooled liquids as functional materials—from plastics and rubbers, to glues and even golf clubs—the nature of the glass transition remains an open question.[4] Much progress has been made in explaining the nonexponential response functions of glasses and supercooled liquids by postulating a spatially heterogeneous distribution of relaxation times in the material.[5] Assuming that the size of these heterogeneous regions increases with decreasing temperature, one can furthermore explain the unusually strong temperature dependence of the relaxation time at the glass transition temperature.[6]

Immediately, the question arises as to how long these dynamic heterogeneities persist in the glass: is the lifetime of these heterogeneities comparable to the structural relaxation time of the glass or is it significantly longer than this so-called α-relaxation time? Experimental results could not disagree more, with some results supporting the former view,[7–10] while other experiments prove the latter.[11–15] Single-molecule experiments are in a unique position to answer this open question. Unlike bulk experiments, they eliminate any averaging over heterogeneities by following the glass dynamics in the vicinity of a single probe molecule, observing one dynamic heterogeneity at a time.

II. EXPERIMENT

In single-molecule spectroscopy, a fluorescent probe is embedded in the matrix of interest at a very low concentration.[16–18] Spin-coating microscope cover slips at 3000 rpm with a solution of poly(vinyl acetate) (about 0.15 g polymer in 10 ml chloroform) with nanomolar concentrations of rhodamine B (molecular weight = 479 g/mol) produce approximately 0.3 μm thick polymer films (thickness determined by ellipsometry) with well-separated dye molecules. We anneal the samples for several hours at 45°C (T_g + 13 K) to remove residual solvent from the polymer and to relax the stress in the film after spin coating. Figure 1 shows the structures of rhodamine B (Aldrich) and poly(vinyl acetate) (Scientific Polymer Products, approx. M_w = 100 kg/mol, corresponding to a degree of polymerization of about 1200 monomers). Poly(vinyl acetate) was chosen for its convenient glass transition temperature of about $T_g = 32$°C.[19]

We use changes in the fluorescence polarization caused by the orientational motion of the single molecule as a

[a]Author to whom correspondence should be addressed. Electronic mail: dbingema@williams.edu.
[b]Present address: San Francisco Estuary Institute, Oakland, California 94621, USA.

 © 2011 American Institute of Physics

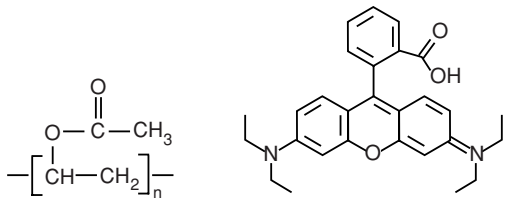

FIG. 1. Structures of the polymer and the probe molecule used in this experiment.

dynamic probe of rearrangements in the polymer environment. The experimental apparatus is built around an inverted microscope (Nikon TE-2000U) equipped with an oil-immersion fluorescence objective (NA = 1.4). A piezo-driven, *xy*-translational stage (Mad City Labs) moves the sample across the laser focus, permitting a maximum scan size of 100 μm by 100 μm. A thermoelectric heater/cooler stage (Melcor), driven by a temperature controller (Alpha-Omega) with a thermistor sensor, maintains the sample temperature constant to within $\pm 0.1^{\circ}$C. A miniature thermocouple element (Omega) continuously monitors the sample temperature close to the laser focus. An enclosure around the microscope eliminates air currents for additional long-term temperature and focus stability.

The 543 nm beam from a cw He-Ne laser (Research Electro-Optics)passes through a 10× beam expander, which increases the laser beam diameter to fill the back aperture of the microscope objective. Neutral density filters attenuate the beam to 20–40 nW, and a quarter-wave plate polarizes the light circularly, eliminating the dependence of the fluorescence intensity on in-plane reorientation of the probe molecule. A band-pass filter (Chroma, D543/10×) removes any unwanted residual discharge emission from the laser light, and a long-pass dichroic mirror (Chroma, Q555LP) redirects the beam into the objective. The microscope objective focuses the excitation beam to a diffraction-limited spot size of 350 nm FWHM (full-width at half-maximum) and collects the fluorescence from the probe molecules. The emission passes through the same long-pass dichroic mirror to separate it from the laser excitation and an additional wide band-pass filter (Chroma, HQ605/90) to remove any residual excitation stray light. A dichroic polarization cube splits the fluorescence into two perpendicular polarization components, which are separately focused by two 100 mm lenses onto the active areas of two single-photon-counting avalanche photodiodes (EG&G, SPAD AQR-13). A multifunction data acquisition card (NI, PCI-6052E) determines the arrival time of every photon (relative to the start of the data acquisition) for both detection channels with 50 ns resolution, monitors the sample temperature, and controls the translational stage through a LABVIEW program. We record all photon arrival times for a full statistical analysis of the fluorescence intensity at a later time. Typical signal intensities in each channel are 5000–10 000 photons/s, allowing for photochemical lifetimes of the probe molecule of up to an hour. We image a portion of the back-reflected excitation light from the laser focus onto a CCD camera to monitor the long-term stability of the laser focus.

The experiments are performed at 32°C, at the glass transition temperature of poly(vinyl acetate). Poly(vinyl acetate) absorbs a small amount of water from the atmosphere,[20] lowering its glass transition temperature from about 43°C for dry poly(vinyl acetate) to about 32°C for poly(vinyl acetate) containing ambient moisture. We performed numerous control experiments to ensure that this plasticizer effect did not alter the results reported here. As the humidity in the laboratory space is constant, the experimental results are very reproducible in repeat experiments at the same temperature. For comparison, we performed experiments with dried poly(vinyl acetate) kept under inert gas atmosphere during all stages of the sample preparation, transfer, and measurement, which yield similar results, however on a much slower time scale, which does not allow us to reach temperatures well above the glass transition temperature on this setup. Control experiments on nonhygroscopic oligo-styrene produce results very similar to those reported here. Finally, we are able to introduce a plasticizer into the oligo-styrene sample by not removing the solvent after spin coating. Only at the highest concentrations of residual solvent does the plasticizer qualitatively alter the results, mainly through the elimination of regions showing the slowest dynamics. Small amounts of residual solvent, comparable to the percentage of water absorbed in poly(vinyl acetate) (Ref. 20) only lead to a shift in the time scale of the dynamics in oligo-styrene without altering the shape of the observed distribution functions.

III. ANALYSIS

The recorded fluorescence intensity in both polarization directions and the ratio of these two fluorescence intensities, as shown in Figs. 2(a) and 2(b) respectively, exhibit sudden changes. While changes in the fluorescence intensity could

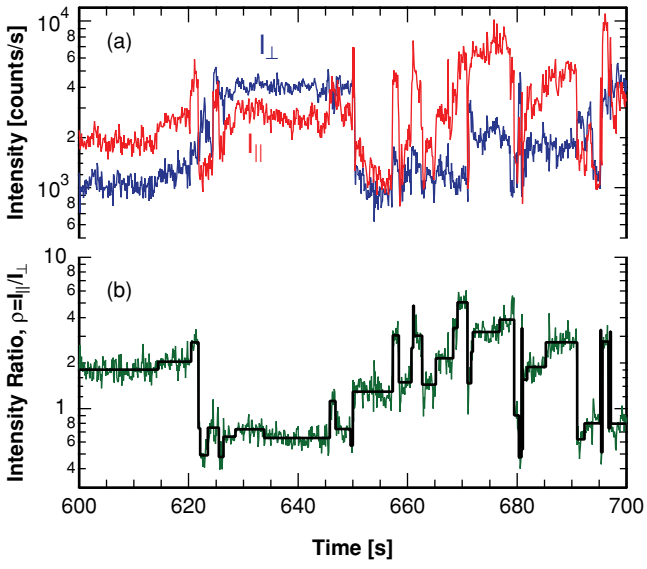

FIG. 2. (a) Intensity of the two polarization components, $I_\parallel$ and $I_\perp$, of the fluorescence emitted by a single rhodamine B molecule embedded in poly(vinyl acetate) at the glass transition temperature. (b) Ratio of the intensity of the two polarization components, $\rho = I_\parallel / I_\perp$, (green) and reconstructed sequence of single-molecule angular jumps (black).

be caused by the probe molecule's photodynamics, such as excursions to the triplet state[21,22] or fluctuations in the fluorescence lifetime due to changes in the probe environment,[23] changes in the ratio of the fluorescence intensity in the two polarization directions, $\rho = I_{\parallel}/I_{\perp}$, indicate reorientations of the probe molecule caused by rearrangements of the polymer matrix.

Single-molecule experiments in glasses are usually analyzed using autocorrelation functions for the recorded trajectories.[14,15,24] As properly averaged autocorrelation functions require a trajectory length exceeding 100 times the decay time,[25] limited photochemical lifetime of the single probe molecules presents a challenge. Here, we use a statistical test to determine the times of the observed sudden changes in the ratio of the fluorescence intensity in the two polarization directions.[26,27] As individual events are detected by this statistical method with no need for averaging, the trajectory length does not affect our analysis.

Details of the analysis method will be published elsewhere.[27] Briefly, we bin photons with a small bin size of 5 ms and calculate the logarithm of the ratio of the intensity in the two detection channels for each bin. Stochastic photon counting noise leads to a near-normal distribution of this measure for any given intensity ratio; we can, therefore, use the standard student t-test to find statistically significant changes in this quantity. As the distribution of the intensity ratio logarithm is not exactly normal, we determine the actual threshold values using the analog of the t-test's p-value at a given confidence level through analysis of simulated photon streams without a break in the intensity ratio (testing for false positives). In the analysis of our experimental results, we choose a conservative 99% level of confidence that in addition has to be surpassed by at least ten consecutive points to guard against false positive identifications. This safeguard limits the shortest detectable wait to about 20 ms and raises the detection threshold, such that our analysis misses some of the smallest angular jumps, especially those separated by short waiting times, but ensures an insignificant fraction (<0.05%) (Ref. 27) of falsely identified jumps.

In separate stochastic simulations of photon streams which feature an intensity ratio break in the center, we determine the fraction of missed jumps (false negatives) as a function of the change in intensity ratio and the number of photons in the sequence.[27] For example, more than 50% of small jumps that change the intensity ratio by less than 25% (change in logarithm by less than 0.1) are still detected in photon sequences of 700 ms length at typical photon rates. Jumps that change the intensity ratio by more than 60% (0.2 change in logarithm) are detected with 50% probability in sections of 200 ms length, and jumps that change the intensity ratio by a factor of 2 (0.3 change in logarithm) are found with 50% probability in sections of 100 ms length, close to the lowest minimum distance between break points required by our safeguard.

We test the sensitivity of our results on jumps missed in the analysis by intentionally excluding those of the already identified jumps, whose change in the intensity ratio falls below a certain threshold. Considering only the remaining "significant" jumps, neither the waiting time distributions nor the correlation function of the logarithm of the intensity ratio, calculated with the reconstructed signals, shows significant deviations from the corresponding results for all identified jumps. For example, the correlation function of the logarithm of the intensity ratio considering only those jumps that change the intensity ratio by more than a factor of 2 (0.3 change in logarithm) still accounts for over 96% of the correlation loss. We would like to add that this threshold excludes over 70% of the identified jumps. Figure 6 shows that the correlation function of the logarithm of the intensity ratio calculated from the original experimental data and from the reconstructed trajectory overlaps almost perfectly, except for the early-time noise peak, which is of course absent in the reconstructed trajectory. These examples show that the results determined from the waiting time sequences are very robust, even though the sequences themselves are not unique and still depend on the noise level or the chosen level of confidence. This analysis approach allows for a dynamic range of 4 orders of magnitude in time, limited only by the photochemical lifetime of the single-molecule probe (about 10^3 s) and the inverse of the average photon rate.

The t-test can only identify one most probable change point in a given sequence of intensity ratios. To find all change points in our experimental trajectory, we systematically test for potential break points in a slowly growing section of the trajectory, starting at the last identified break point. After detecting a new probable break point, we double-check all previously identified change points to either confirm or reject them at the chosen level of confidence. This approach eventually yields a time sequence of most likely intensity ratio change points. We calculate the intensity ratio between two identified change points from the number of photons recorded between these two times in each detection channel.

Figure 2(b) overlays an example of such a reconstructed sequence of wait times and step sizes onto the original experimental result. From this reconstructed sequence, we can determine the individual distributions of waiting times and jump sizes, as well as all autocorrelations and cross correlations between these two quantities. In bulk experiments only a small fraction of this information is accessible and most of it only through complex higher-order nonlinear spectroscopic techniques.[28,29] In this paper, we focus entirely on the waiting time portion of our results and leave the discussion of jump sizes for a subsequent paper.

IV. RESULTS

A. Qualitative comparison of trajectories

Figure 3(b) compares trajectories of the fluorescence intensity ratio, ρ, for ten single probe molecules with the longest trajectories. These molecules are located at well-separated sites in the same polymer sample. In each single-molecule trajectory periods of fast and slow reorientations are noticeable, indicative of heterogeneous dynamics. Careful inspection also shows that none of the periods with fast motion appears to be longer than the longest of the waiting times noticeable in the trajectories, suggesting that the lifetime of the heterogeneities cannot be longer than the waiting

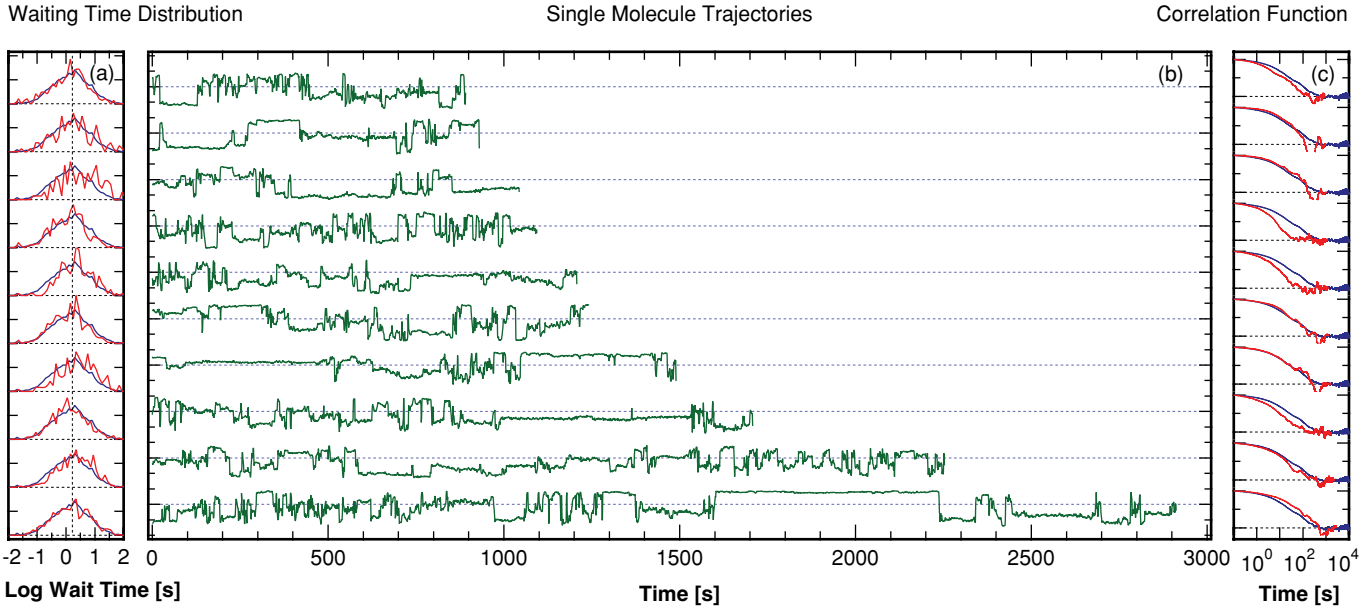

FIG. 3. The ten longest single-molecule trajectories recorded with rhodamine B in poly(vinyl acetate) at the glass transition temperature. (a) Comparison of the probability distributions for the logarithm of the waiting time between two angular jumps for each individual single molecule (red) and for all molecules in the sample combined (blue). (b) Logarithm of the ratio of the fluorescence intensity in the two polarization directions, $\log(\rho)$, with $\rho = I_{\parallel} / I_{\perp}$. (c) Comparison of the orientational correlation functions for each individual single molecule (red) with the correlation function averaged over the entire sample (blue).

times between jumps of the probe molecule. All molecules show similar patterns of slow and fast motions on comparable time scales, which suggest that any spatial heterogeneities in the glass dynamics as probed with different single molecules must be short lived as well.

To analyze these results quantitatively, we first calculate the distribution of waiting times between jumps. We focus on the logarithm of the waiting times to take into consideration the significant broadening of the waiting time distribution due to heterogeneities. Figure 4(a) shows that there is no statistically significant difference between the waiting time distribution for the single probe molecule with the longest recorded trajectory (red line) and the waiting time distribution for all molecules in the sample combined (blue line). This conclusion in fact holds for all molecules depicted in Fig. 3(b) as shown in Fig. 3(a) by the comparison of each molecule's waiting time distribution to the waiting time distribution of all molecules combined. This again indicates a lack of variation between different probe molecules, supporting the inference about the absence of long-lived spatial heterogeneities.

The time scale of single-molecule reorientation is often determined from its orientational correlation function. However, the orientational correlation time (along with visual impressions of single-molecule trajectories) is strongly dependent on the presence or absence of rare long waiting times. For example, the lack of any long waiting times for molecules 4 and 5 (counting from the top) in Fig. 3 leads to slightly shorter correlation times for those two molecules as shown by the comparison of each molecule's correlation function for the logarithm of the intensity ratio to the average correlation function in Fig. 3(c). We discuss below that these deviations are most likely the result of poor sampling statistics of rare events in short single-molecule trajectories and no indication of long-lived heterogeneities.

B. Waiting time correlation

The dependence of one waiting time between two probe molecule angular jumps on the previous waiting time provides a measure for the lifetime of the heterogeneities. In the case of homogeneous dynamics, subsequent waiting times are uncorrelated. For very long heterogeneity lifetimes, a long waiting time is most likely caused by a slow environment and will probably be followed by another long waiting time, while a short waiting time is most likely followed by another short waiting time. For heterogeneous dynamics subsequent waiting times are, therefore, correlated.

The contour plots in Figs. 4(c) and 4(e) and the points in Fig. 4(b) show the dependence between subsequent waiting times for a single molecule (red) and all molecules in the sample combined (blue). Again, we find no statistically significant difference between the results for a single molecule and the results for the ensemble average. The point cloud is elongated along the diagonal leading to a correlation of $r = 0.26$ between the logarithm of subsequent waiting times. The correlation for the logarithm of waiting times that are separated by an increasing number of jumps decreases quickly as illustrated with the autocorrelation function in Fig. 5(a). Following standard time-series analysis we calculate the partial autocorrelation function, which reveals how far the effect of a single jump can be noticed. To illustrate this concept with an example, a time series with a correlation between subsequent points of, say, 0.50 automatically implies a correlation between second neighbors of at least 0.25. If, however, the actual correlation between second neighbors is 0.30, then the partial correlation between second neighbors is the difference, or 0.05. The partial autocorrelation, hence, reflects the unique contribution of the nth neighbor correlation beyond any cascaded lower-order correlation effects. Figure 5(b) shows that

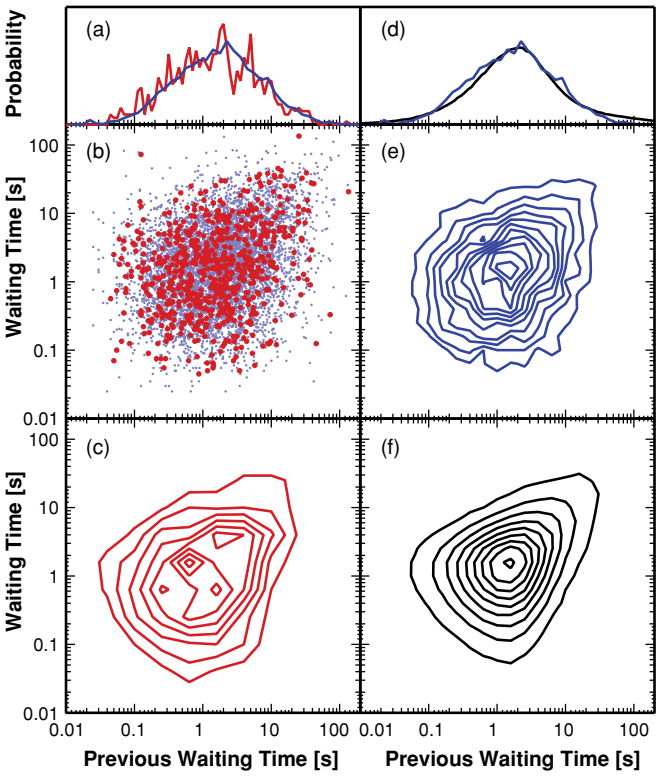

FIG. 4. Comparison of the waiting time correlations for one single molecule and for all molecules combined with the result of a simulation with the proposed model for glass dynamics. (a) and (d) Comparison of the probability distribution for the logarithm of the waiting time between two single-molecule angular jumps for a single probe molecule (red), for all molecules combined (blue), and for the results of the model simulations (black). (b) Correlation of two subsequent waiting times in between angular jumps for a single molecule (red) and all molecules combined (blue). (c), (e), and (f) Contour plot for the correlation between subsequent waiting times for the same single molecule (c), all molecules combined (e), and the result of the model simulation (f).

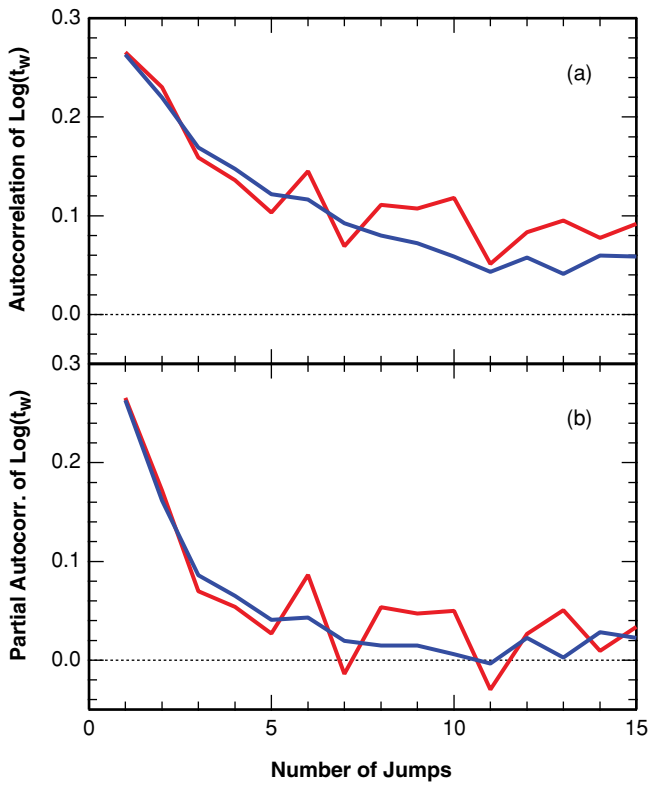

FIG. 5. (a) Autocorrelation function and (b) partial autocorrelation function for the logarithm of the waiting time, t_w, as a function of the number of jumps separating the two waiting times calculated for a single molecule (red), for all molecules combined (blue).

waiting periods more than about six angular jumps apart do not add any more statistically significant contribution to the correlation between waiting times. The small but significant correlation of consecutive waiting times confirms our earlier qualitative inference that the dynamics in the sample is heterogeneous, while the fast decay of the partial autocorrelation function confirms that these heterogeneities are short lived.

C. Heterogeneity correlation time

Considering glass dynamics as a sequence of activated barrier-crossing events and assuming Arrhenius-type behavior for each individual rearrangement, we can use the logarithm of the waiting time between jumps as a statistical measure of the barrier height at the moment of the glass rearrangement. We consider this estimated barrier height an identifier for an individual heterogeneity, which allows us to determine the lifetime of heterogeneities from the sequence of waiting times determined in our analysis. The waiting time sequence can only produce an estimate for the barrier height at the time of each jump; hence we assume that the unknown barrier height in between jumps is constant and equal to the height estimated from the logarithm of the waiting time leading up to the jump time. The actual barrier most likely also fluctuates between jumps; we, therefore, will only be able to determine an upper estimate for the heterogeneity lifetime.

Based on these assumptions, we calculate the correlation function of the logarithm of the waiting time as a function of time (as opposed to as a function of the number of jumps separating the waiting times as done in Sec. IV B).Even though the waiting times are only exponentially distributed statistical estimates of the barrier heights, correlating such statistical quantities still determines the correlation function of the underlying control parameter,[30] in this case the barrier height. Figure 6 compares the correlation function for the logarithm of the waiting times (green) to the correlation function of the logarithm of the intensity ratio calculated for all trajectories in the sample combined (blue). The functional values for log $\rho = \log (I_\parallel/I_\perp)$ correlated here are very similar to the linear dichroism, LD $= (I_\parallel - I_\perp) / (I_\parallel + I_\perp)$, which is traditionally used in single-molecule microscopy; however, the logarithm of the intensity ratio maintains a near-normal noise characteristic across the range of possible functional values. A fit of the correlation function of the logarithm of the intensity ratio with a stretched exponential function, $f(t) = \exp[-(t/\tau)^\beta]$, yields a stretching parameter of $\beta = 0.62$ and a correlation time of $\tau_{\text{orient}} = 90$ s. The same fit to the correlation function of the barrier height fluctuations gives a similar stretching parameter of $\beta = 0.60$ and a correlation time of $\tau_{\text{het}} = 32$ s. To test the sensitivity of this result on the detection limit of our analysis method, we intentionally exclude

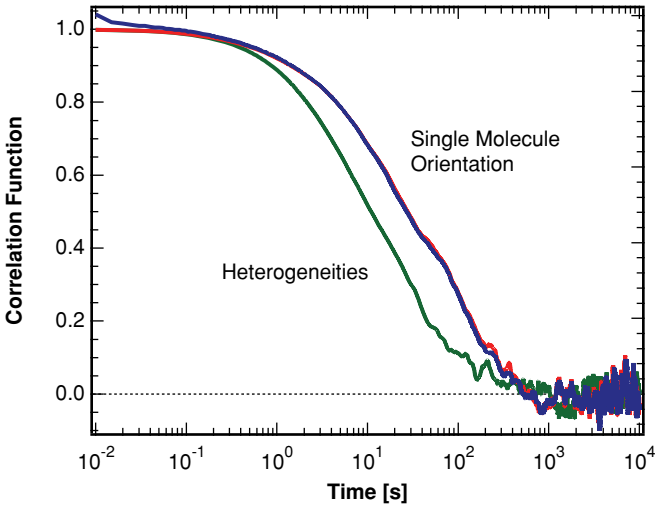

FIG. 6. Comparison of the ensemble averaged orientational correlation function of the single-molecule orientation as calculated with the original data (blue) and with the trajectory reconstructed from the jump times found in the analysis (red). Correlation of the logarithm of the waiting time between subsequent jumps as an estimate for the correlation of the fluctuations of the activation barrier for glass rearrangements (green).

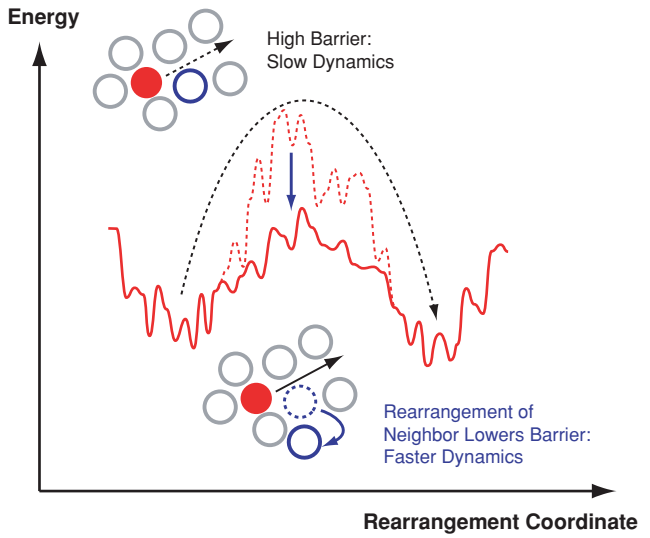

FIG. 7. Schematic illustration of the proposed model for glass dynamics. The barrier for an activated local glass rearrangement in one region is altered by rearrangements in a neighboring region.

all small angular jumps that change the intensity ratio by less than 25% in the calculation of the correlation function of the logarithm of the waiting time. This increases our result for the lifetime of the heterogeneities slightly to $\tau_{\text{het}} = 38$ s, while the stretching parameter does not change.

V. MODEL FOR GLASS DYNAMICS

Here, we propose a simple model for the glass dynamics that is consistent with the statistics of the sequence of waiting times determined through our analysis.

A. Description of model

The abruptness of the angular jumps as shown in Fig. 2(b) suggests that we can picture glass dynamics in terms of fast, barrier crossing, rearrangement events that are separated by waiting periods without any significant structural changes. This view is supported by molecular dynamics studies.[31] Inspired by the facilitation approach,[32] we assume that the activation barrier for a rearrangement in one region in the glass is altered whenever a neighboring region rearranges, as illustrated in Fig. 7. Thus, in this model we assume that the fluctuations of the barrier heights, which we interpret as the dynamics of the heterogeneities, follow the dynamics of the glass itself.

To simulate this model numerically, we randomly pick a new barrier height from an exponential distribution whenever a neighboring region experiences a rearrangement. The choice of an exponential distribution for the barrier heights is guided by results from our own molecular dynamics simulations on a model polymer. A Gaussian distribution of barrier height fluctuations[33] did not yield satisfactory agreement with our results. Consistent with this fluctuating barrier, we randomly choose waiting times for activated rearrangement events in the region of interest. Using the resulting sequence of rearrangement times as a sample of the dynamics of a neighboring, barrier changing, region in the subsequent run, we repeat these simulations a few times until they converge. Adjustable model parameters are an average time scale and the decay constant for the exponential distribution of the fluctuating barrier heights.

B. Results of model calculations

The proposed model reproduces the statistics of the experimentally observed waiting time sequences very well as shown by the contour plot of the simulated waiting time correlation in Fig. 4(f) and by the black line representing the simulated waiting time distribution in Fig. 4(d). The model for the glass dynamics also allows us to simulate intensity ratio trajectories, as shown in Fig. 8, which are comparable to the experimental trajectories shown in Fig. 3. Here, we calculate the waiting times between jumps with the glass dynamics model outlined above. Angular jump sizes of the simulated trajectories stem from random walks on a sphere with exponential jump size distribution. Through analysis of simulated data[27] and comparison to our single molecule results, we find that we do not need to assume that waiting times and jump sizes are correlated. We subsequently calculate intensities of the two polarization directions for each orientation accounting for the high numerical aperture of the microscope objective,[34] randomly pick photon arrival times with Poisson waiting time distribution consistent with these intensities in the two detection channels and finally bin the photons as done in the analysis of the experiment. These binned intensities are shown in Fig. 8.

VI. DISCUSSION

The model assumption that the dynamics of the heterogeneities is identical to the dynamics of the glass itself

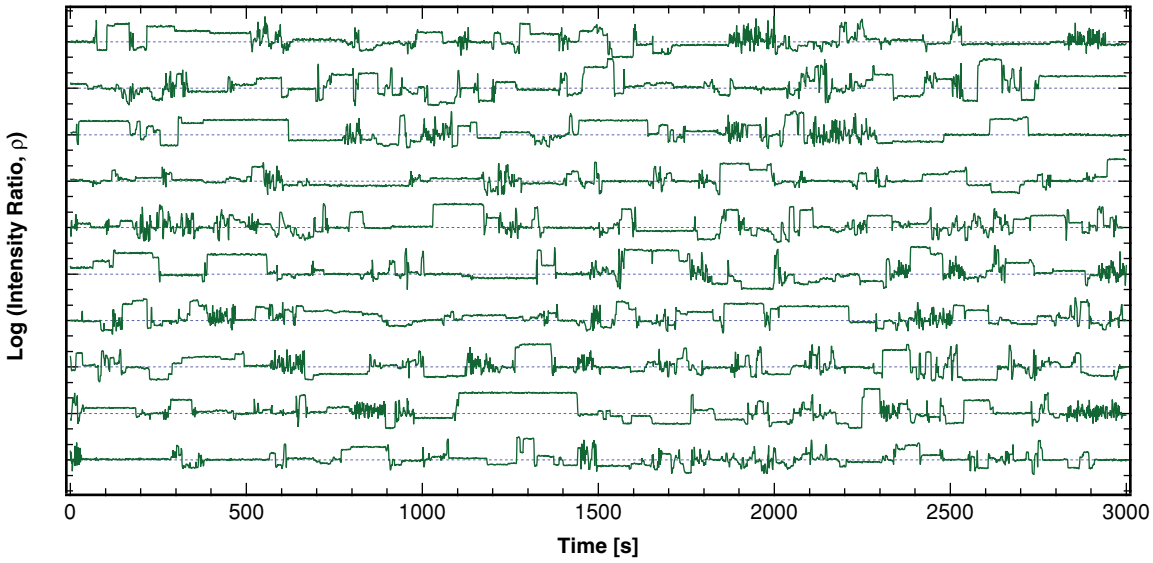

FIG. 8. Ten trajectories calculated from waiting time sequences simulated with the proposed model for the glass dynamics in combination with an uncorrelated exponential jump size distribution as described in the text.

produces waiting time sequences that are statistically indistinguishable from our experimental results. This assumption implies that the lifetime of the heterogeneities is identical to the structural relaxation time of the glass, as observed previously with multidimensional nuclear magnetic resonance experiments,[7–9] atomic force microscopy,[10] and dielectric hole-burning experiments.[8] We would like to add that the proposed model for the glass dynamics also predicts changes to the width of emission spectra similar to those observed experimentally.[11]

For a model-free determination of the ratio between heterogeneity lifetime and structural correlation time, we turn to the correlation time of the fluctuations of the height of the activation barrier for local rearrangements, $\tau_{\text{het}} = 32$ s, as estimated from the logarithm of the waiting times between single-molecule jumps. In order to compare this lifetime of the heterogeneities to the structural relaxation time of the sample, we first consider the correlation function of the logarithm of the intensity ratio, which is comparable to the correlation function of the linear dichroism, with a correlation time of $\tau_{\text{orient}} = 90$ s. The heterogeneity lifetime is about three times shorter than the orientational correlation time in contrast to results from other single molecule experiments,[14,15] which, using other approaches to determine the heterogeneity lifetime, find heterogeneity lifetimes 15 times and 25 times longer than the orientational correlation time for the single molecule, or 300 times and 200 times slower than the structural relaxation time, τ_α, respectively.

Orientational correlation functions for probe molecules depend on the size of the probe molecule,[35,36] with larger probe molecules leading to slower and more exponential correlation functions. The stretching exponent in our single-molecule correlation function, $\beta_{\text{orient}} = 0.62$, is significantly larger than the one observed in dielectric experiments,[37] $\beta_{\text{dielectric}} = 0.39$, therefore the single molecule orientational correlation time, $\tau_{\text{orient}} = 90$ s, is most likely significant longer than the structural relaxation time of the sample at this temperature. We can estimate the factor between orientational correlation time and structural relaxation time for our host/guest combination from single molecule experiments performed on carefully dried samples, for which the α-relaxation time is known from dielectric experiments. The single-molecule orientational correlation function we record for rhodamine B in carefully dried poly(vinyl acetate) at its glass transition temperature of 43°C is fit well with a stretching exponent of $\beta_{\text{orient,dry}} = 0.53$ and a time scale of $\tau = 54$ s, giving an orientational correlation time of $\tau_{\text{orient,dry}} = 97$ s. From dielectric relaxation experiments[38] on poly(vinyl acetate) with a comparable molecular weight of 170 kg/mol, we interpolate for the same temperature a relaxation time of $\tau_{\alpha,\text{dry}} = 2.7$ s. The orientational correlation time, $\tau_{\text{orient,dry}}$, in dry poly(vinyl acetate) at the glass transition temperature is, therefore, 36 times longer than the structural relaxation time, $\tau_{\alpha,\text{dry}}$, for our host/guest combination. Assuming that the same factor also applies for the same probe molecule in ambient moisture poly(vinyl acetate) at its glass transition temperature of 32°C, we can estimate from the orientational correlation time of $\tau_{\text{orient,ambient}} = 90$ s a structural relaxation time of $\tau_{\alpha,\text{ ambient}} = 2.5$ s at this temperature.

The comparison between the thus estimated structural relaxation time $\tau_{\alpha,\text{ ambient}} = 2.5$ s and the determined upper limit for the heterogeneity lifetime $\tau_{\text{het}} = 32$ s shows that the measured heterogeneity lifetime is about 13 times longer than estimated structural relaxation times of the sample at the glass transition temperature. Given that the experimental result for the heterogeneity lifetime should be considered an upper estimate for the true lifetime of the heterogeneities and keeping in mind the uncertainties caused by the approximations required in this estimate, we do not consider this result a contradiction to the prediction of the proposed model, that the lifetime of the heterogeneities is identical to the structural relaxation

time of the glass. In fact, the model even goes one step further by equating not just the time scales, but rather the dynamics of the heterogeneities and the dynamics of the glass itself.

Heterogeneity lifetimes much longer than the structural relaxation time, as observed in optical bleaching experiments,[12,13] would not be visible in individual single-molecule trajectories since their length are limited by photobleaching of the probe molecule. Nevertheless, such long-lived heterogeneities should lead to qualitatively different trajectories for different probe molecules in the same sample. No such differences are apparent in Fig. 3(b), nor are there any statistically significant differences between the cumulative waiting time sequence and the waiting time sequence for the individual molecules [Figs. 3(a), 4, and 5]. However, some differences are noticeable in Fig. 3(c) between the correlation functions of the logarithm of the intensity ratio for individual molecules and the corresponding correlation function for the ensemble average. We believe that these deviations should not be mistaken for long-lived heterogeneities[14] but that they are simply a consequence of poor statistics for the longest waiting times. Correlation functions, like bulk experiments, intrinsically time weight the dynamics as they are statistically more likely to sample regions characterized by long waiting times. We find that the broad distribution of relaxation times caused by the heterogeneities even leads to significant fluctuations in the regular, not weighted, waiting time average, which take on the order of 10^3 s to converge in both our experimental results and model simulations. We, therefore, argue that this slow convergence in combination with the high sensitivity of correlation functions to the longest waiting times is the reason for the deviations of the individual molecule's orientational correlation functions from the ensample average as shown in Fig. 3(c) and not a sign of long-lived heterogeneities.

Recently, heterogeneity lifetimes about 200 times longer than the structural relaxation time were reported for glycerol at $T_g + 14$ K using rubrene as a single probe molecule.[15] In contrast to the sudden angular jumps shown in Figs. 2(b) and 3(b), the single-molecule trajectories for glycerol were diffusive, which might indicate a different mechanism for the structural relaxation of this hydrogen-bonded molecular glass former compared to the polymeric glass former investigated here.

Probe molecules have been used extensively to study the dynamics in glasses.[5] There are limitations to this approach, most notably the probe molecule's size, which leads to slower and more exponential orientational correlation functions compared to bulk dielectric experiments.[35,36] However, probe molecules report truthfully on, for example, the temperature dependence of the glassy dynamics, albeit with shifted correlation times. The insertion of a rather large probe molecule such as rhodamine B, whose largest dimension (approximately 0.9 nm) approaches the length scale of dynamic heterogeneities,[39–41] raises the question whether the probe molecule changes the local environment and its dynamics in our single molecule experiment. Given the general success of using probe molecules to measure bulk glass or liquid dynamics in a variety of experiments, we are confident that these dye molecules also probe representative samples of local dynamics in single molecule experiments. Additional single molecule experiments with other probe molecules in our setup show qualitatively similar results; however, the variation of molecular weights (as a measure of the probe molecule size[36]) of suitable laser dyes is limited. Experiments with pyrromethene 597 (molecular weight = 486 g/mol), for example, yield statistical measures, correlations, and distribution functions that are comparable to those from experiments with rhodamine B (molecular weight = 479 g/mol) at the same temperature. We are, therefore, confident that probe molecule specific interactions with the polymer do not affect the recorded dynamics. In the light of the vast body of experiments using probe molecules to study bulk glass dynamics, we are convinced that the single molecule results reported here are representative of the glass dynamics of a single local environment.

In this paper, we present a different approach to investigate the dynamics in glasses, namely, utilizing waiting time sequences and waiting time distributions of individual single-molecule jumps instead of their orientational correlation functions, which are usually used in single-molecule spectroscopy and bulk spectroscopic techniques. Waiting time sequences, on the other hand are common in theoretical approaches, for example continuous time random walk simulations.[42] Even though the waiting time sequences found for our experimental data are not unique, the results determined with them are very robust. Most importantly, this approach avoids the shortcomings of the limited trajectory length in single-molecule spectroscopy. Given the broad distribution of waiting times, truncated trajectories exhibit poor statistics for the long waiting times, leading to large fluctuations of correlation times due to the large weight of these long waiting times in the correlation function average. Waiting time distributions are not sensitive to these statistical fluctuations in the frequency of rare events, which constitute only a minor contribution to the total sample. On the other hand, as these long waiting times dominate the correlation function and bulk properties, they also hold the key to understanding the dramatic slowdown experienced at the glass transition. The investigation of waiting times, as pursued in this work, might therefore offer a second, complementary, point of view in the study of glass dynamics.

The proposed model for the glass dynamics does not specify the identity of the "region" that experiences a transition event. In our experiment, we observe angular jumps of a probe molecule and we interpret those as evidence for structural rearrangements of the polymer in the vicinity of the probe. One possible identity of this region is the coordinated motion of several monomer units in possibly several neighboring polymer chains. Such a collective motion of monomer units moving together could be understood as an example of a cooperatively rearranging region.[6,43,44] Considering only a single neighboring region, as done in the proposed model, is certainly an oversimplification. Kinetically constrained models of the glass dynamics[45] in fragile glass formers require at least two facilitating neighbors out of typically four to six nearest neighbors. Coordination numbers in Lennard-Jones liquids even reach values of 11 or 12. However, despite these simplifications, we find good agreement between experiment and simulations with the proposed model of the glass dynamics.

VII. CONCLUSION

Single rhodamine B probe molecules in poly(vinyl acetate) at the glass transition temperature reorient with sudden movements consistent with activated glass dynamics. Upon qualitative inspection, individual trajectories do not display long periods of preferentially fast or slow motion, ruling out long-lived heterogeneities. Also, no qualitative differences are noticeable in the dynamics of well-separated probe molecules in the same sample, again indicating a lack of long-lived spatial heterogeneities. Identifying each angular jump through a statistical search for break points in the logarithm of the ratio of two perpendicular polarization components of the recorded fluorescence, we reconstruct the sequence of glass rearrangement events in the vicinity of the probe molecule. Time-series analysis of this sequence of waiting times reveals a significant, but short lived, correlation, confirming the qualitative assertion of short-lived heterogeneities. We determine an upper limit for the heterogeneity lifetime with the correlation function of the logarithm of the waiting times between single-molecule jumps and find a correlation time about 13 times longer than the estimated structural relaxation time of the polymer at this temperature. We propose a model for glass dynamics that describes the dynamics of heterogeneities as fluctuations of the barrier for glass rearrangements. Randomly changing this barrier in numerical simulations whenever a glass rearrangement event occurs in a neighboring region, that is, equating the dynamics of the heterogeneities with the dynamics of the glass itself, we can successfully reproduce the statistics of the experimentally recorded sequence of waiting times. The strong resemblance between experimental and simulation results in Figs. 3 and 8, respectively, as well as in Fig. 4, suggests that the proposed glass dynamics model captures some of the fundamental aspects of the heterogeneous dynamics in glasses and supercooled liquids.

ACKNOWLEDGMENTS

This work was made possible through National Science Foundation Grant No. CHE-0749863.

[1]P. G. Debenedetti and F. H. Stillinger, Nature **410**, 259 (2001).
[2]M. D. Ediger, C. A. Angell, and S. R. Nagel, J. Phys. Chem. **100**, 13200 (1996).
[3]C. A. Angell, Science **267**, 1924 (1995).
[4]P. W. Anderson, Science **267**, 1615 (1995).
[5]M. D. Ediger, Annu. Rev. Phys. Chem. **51**, 99 (2000).
[6]G. Adam and J. H. Gibbs, J. Chem. Phys. **43**, 139 (1965).
[7]R. Böhmer, G. Diezemann, G. Hinze, and H. Sillescu, J. Chem. Phys. **108**, 890 (1998).
[8]B. Schiener, R. Böhmer, A. Loidl, and R. V. Chamberlin, Science **274**, 752 (1996).
[9]U. Tracht, A. Heuer, S. A. Reinsberg, and H. W. Spiess, Appl. Magn. Reson. **17**, 227 (1999).
[10]E. V. Russell and N. E. Israeloff, Nature **408**, 695 (2000).
[11]R. Richert, J. Non-Cryst. Solids **307**, 50 (2002).
[12]C. Y. Wang and M. D. Ediger, J. Phys. Chem. B **103**, 4177 (1999).
[13]C. Y. Wang and M. D. Ediger, J. Chem. Phys. **112**, 6933 (2000).
[14]L. A. Deschenes and D. A. Vanden Bout, J. Phys. Chem. B **106**, 11438 (2002).
[15]S. A. Mackowiak, T. K. Herman, and L. J. Kaufman, J. Chem. Phys. **131**, 244513 (2009).
[16]W. E. Moerner, J. Phys. Chem. B **106**, 910 (2002).
[17]W. E. Moerner and M. Orrit, Science **283**, 1670 (1999).
[18]X. S. Xie and J. K. Trautman, Annu. Rev. Phys. Chem. **49**, 441 (1998).
[19]D. R. Lide, *CRC Handbook of Chemistry and Physics*, 84th ed., Chemical Rubber Company Press, Boca Raton, FL, 2003–2004.
[20]G. D. Smith, F. Liu, R. W. Devereaux, and R. H. Boyd, Macromolecules **25**, 703 (1992).
[21]T. Basche, J. Lumin. **76–77**, 263 (1998).
[22]T. Plakhotnik, E. A. Donley, and U. P. Wild, Annu. Rev. Phys. Chem. **48**, 181 (1997).
[23]R. A. L. Vallee, N. Tomczak, G. J. Vancso, L. Kuipers, and N. F. van Hulst, J. Chem. Phys. **122**, 114704 (2005).
[24]A. N. Adhikari, N. A. Capurso, and D. Bingemann, J. Chem. Phys. **127**, 027732 (2007).
[25]D. Bingemann, Chem. Phys. Lett. **433**, 234 (2006).
[26]L. P. Watkins and H. Yang, J. Phys. Chem. B **109**, 617 (2005).
[27]R. M. Allen and D. Bingemann, "*Identification of Intensity Ratio Break Points in Ratiometric Single Molecule Spectroscopy*", J. Phys. Chem. B (2011) (submitted).
[28]K. Schmidt-Rohr and H. W. Spiess, *Multidimensional Solid-State NMR and Polymers* (Academic, London, 1994).
[29]S. Mukamel, *Principles of Nonlinear Optical Spectroscopy* (Oxford University Press, New York, 1995).
[30]H. Yang and X. S. Xie, J. Chem. Phys. **117**, 10965 (2002).
[31]A. Heuer, J. Phys. Condens. Matter **20**, 373101 (2008).
[32]Y. Jung, J. P. Garrahan, and D. Chandler, J. Chem. Phys. **123**, 084509 (2005).
[33]M. Dzero, J. Schmalian, and P. G. Wolynes, Phys. Rev. B **80**, 024204 (2009).
[34]J. T. Fourkas, Opt. Lett. **26**, 211 (2001).
[35]M. T. Cicerone, F. R. Blackburn, and M. D. Ediger, J. Chem. Phys. **102**, 471 (1995).
[36]M. Yang and R. Richert, Chem. Phys. **284**, 103 (2002).
[37]L. E. Walther, N. E. Israeloff, E. V. Russell, and H. A. Gomariz, Phys. Rev. B **57**, 15112 (1998).
[38]W. Heinrich and B. Stoll, Colloid Polym. Sci. **263**, 873 (1985).
[39]S. A. Reinsberg, X. H. Qiu, M. Wilhelm, H. W. Spiess, and M. D. Ediger, J. Chem. Phys. **114**, 7299 (2001).
[40]X. H. Qiu and M. D. Ediger, J. Phys. Chem. B **107**, 459 (2003).
[41]U. Tracht, M. Wilhelm, A. Heuer, H. Feng, K. Schmidt-Rohr, and H. W. Spiess, Phys. Rev. Lett. **81**, 2727 (1998).
[42]J. P. Garrahan, R. L. Jack, V. Lecomte, E. Pitard, K. van Duijvendijk, and F. van Wijland, J. Phys. A: Math. Theor. **42**, 075007 (2009).
[43]R. Richert and C. A. Angell, J. Chem. Phys. **108**, 9016 (1998).
[44]M. Vogel, B. Doliwa, A. Heuer, and S. C. Glotzer, J. Chem. Phys. **120**, 4404 (2004).
[45]F. Ritort and P. Sollich, Adv. Phys. **52**, 219 (2003).